Letter

Experimental evidence of exact E(5) symmetry in ^{82}Kr

S. Rajbanshi,[1,*] S. Bhattacharya,[2] R. Raut,[3,†] R. Palit,[4] Sajad Ali,[5] Rajkumar Santra,[6,7] H. Pai,[6] F. S. Babra,[4] R. Banik,[7,8] S. Bhattacharyya,[7,9] P. Dey,[4] G. Mukherjee,[7,9] Md. S. R. Laskar,[4] S. Nandi,[7,9] T. Trivedi,[2] S. S. Ghugre,[3] and A. Goswami[6]

[1]*Presidency University, Kolkata 700073, India*
[2]*Department of Pure and Applied Physics, Guru Ghasidas Vishwavidyalaya, Bilaspur 495009, India*
[3]*UGC-DAE-Consortium for Scientific Research, Kolkata 700098, India*
[4]*Tata Institute of Fundamental Research, Mumbai 400005, India*
[5]*Government General Degree College at Pedong, Kalimpong 734311, India*
[6]*Saha Institute of Nuclear Physics, 1/AF, Bidhannagar, Kolkata 700064, India*
[7]*Homi Bhabha National Institute, Training School Complex, Anushakti Nagar, Mumbai 400094, India*
[8]*Institute of Engineering and Management, Saltlake Sector V, Kolkata 700091, India*
[9]*Variable Energy Cyclotron Center, Kolkata 700064, India*

(Received 13 October 2020; revised 26 July 2021; accepted 24 August 2021; published 7 September 2021)

The low-lying positive-parity structures of ^{82}Kr have been investigated following their population in the ^{76}Ge(^{9}Be, $3n$) reaction at $E_{lab} \approx 31$ MeV and using a large array of Compton suppressed HPGe clovers as the detection setup. Apart from other spectroscopic measurements, level lifetimes of the states have been extracted using the Doppler shift attenuation method. The level energies and the associated transition probabilities exhibit superlative overlap with the calculations in the framework of the interaction boson approximation and the E(5) model. The ^{82}Kr nucleus, thus, exemplifies the critical point of phase (shape) transition from the U(5) (spherical vibrator) to the O(6) (γ-soft rotor) paradigms of nuclear structure.

DOI: 10.1103/PhysRevC.104.L031302

The investigation of the phase-transitional properties of physical systems is known to be of pertinence in natural science. One of the challenges in such pursuits pertains to the rapid change in the order parameter with variation in the control parameter at the point of phase transition that makes it obscure to unambiguously identify the latter. In nuclei, the phase transitions will occur at zero temperature and correspond to the change in the equilibrium deformation or ground-state symmetry of the system with variation in the number of nucleons that acts as the control parameter [1,2].

As far as shapes or deformations of nuclei are concerned, they can principally be a spherical harmonic vibrator [3], an axially symmetric deformed rotor [4], or a γ unstable (axially asymmetric) rotor [5]. These constitute the idealized limits of nuclear shapes that have been encoded in the framework of the interacting boson approximation (IBA) and have been identified to correspond to different dynamical symmetries: The spherical vibrator is associated with U(5), the axially symmetric rotor with SU(3) and the γ-soft rotor with O(6) [6]. Each of these symmetries has characteristic experimental signatures, such as the ratio of the excitation energies of the first 4^+ and 2^+ states $R_{4/2}$, that is 2.0 for U(5), 3.33 for SU(3), and 2.5 for O(6).

Furthermore, the (phase) transition from one of these paradigms into another is characterized by critical point symmetries (CPS) as invoked by Iachello for a simple parameter-free analytical treatment of transitional nuclei [7,8]. The CPS associated with the transition from the spherical vibrator to the axially symmetric rotor is $X(5)$ [7] whereas that with a spherical vibrator to a γ-soft rotor is E(5) [8]. The transitional character is typically quantified through experimental observables, such as the aforementioned ratio of excitation energies as well as the ratio of transition probabilities, eventually elaborated in this paper. Recently, the relativistic mean-field theory has been applied to probe the $X(5)$ symmetry in ^{148,150,152}Sm [9] and E(5) in Ti isotopes [10] whereas, most proximal manifestations of E(5) symmetry has been identified in ^{134}Ba [11], ^{130}Xe [12], ^{104}Ru [13], and ^{102}Pd [14]. These investigations have not reported the levels above the first excited 0^+ state which is crucial for the understanding of the E(5) behavior in nuclei. The position of this excited 0^+ state vary along with the U(5) to O(6) transition [15–17]. For U(5), this state has a two-phonon character with high B(E2) rate to the one phonon 2_1^+ level. In the O(6) limit this level becomes very high in excitation energy and the B(E2) transition strength to the 2_1^+ state is forbidden. In contrast, the second excited 0^+ level preserves its three-phonon character across the entire U(5) to O(6) path [15].

It may be noted that all the above-mentioned findings on E(5) symmetry are for stable nuclei with $A > 100$. The lone exception is the proposition of E(5) symmetry in ^{58}Cr [18]

*subhphy@gmail.com
†rraut@alpha.iuc.res.in

that caters to an impetus for investigating phase transitions in the neighboring nuclei ($A < 100$) as well. The nuclei in the $A \approx 80$ region lie between the shell closure at $N = 50$ that exhibits sphericity [19–22], and the subshell gap at $N = 40$, around which triaxiality has been established [23–26]. The $R_{4/2}$ and $R_{6/2} \equiv \mathrm{E}(6_1^+)/\mathrm{E}(2_1^+)$ values of ^{82}Kr ($Z = 36$, $N = 46$) are 2.35 and 3.76, respectively [27]. These values lie around the midway between U(5) and O(6) limits, thus, making this nucleus a potential candidate for observing E(5) symmetry characterized by $R_{4/2} = 2.19$ and $R_{6/2} = 3.53$ for systems having six bosons.

In this Letter, we report the first evidence of E(5) dynamical symmetry and second-order phase transition from U(5) to O(6) manifested in ^{82}Kr as the maiden instance of such observation in the $A \approx 80$ region. Evidence of E(5) dynamical symmetry in ^{82}Kr is strongly supported by the maiden observation of repetition of the ground-state structure above first excited 0^+ state at 2172 keV and measurement of the B(E2) strengths of the deexciting transitions therefrom. The E(5) dynamical symmetry of this nucleus has been established by comparing the measured energies and transition strengths with the theoretical calculations.

Excited states of ^{82}Kr were populated using the ^{76}Ge(^{9}Be, $3n$) reaction at $\mathrm{E_{lab}} \approx 31$ MeV. The target was 4.2 mg/cm^2 ^{76}Ge (99% enriched) on a 10.8-mg/cm^2-thick lead backing. The latter was positioned to face the beam, before the target, so as to degrade the beam energy from $\mathrm{E_{lab}} =$ 37 MeV to the aforementioned value. The technique incurred an uncertainty of $\approx$0.2 MeV [28] in the beam energy at the target-backing interface but did not significantly impact the velocity (v) of the recoiling nuclei ($v/c \approx 0.9\%$), that would be of pertinence in the level lifetime analysis. The ^{9}Be beam was delivered by the Pelletron Linac Facility at the TIFR, Mumbai. The Indian National Gamma Array (INGA), then consisting of 14 Compton-suppressed HPGe clover detectors positioned at 40°(2), 90°(4), 115°(2), 140°(3), and 157°(3) with respect to the beam axis (the number in the parentheses is the detector numbers at the respective angles) [29] was employed to detect the deexciting γ rays. Time-stamped list mode data were acquired under the condition of (γ-γ) coincidence multiplicity $\geqslant 2$. Of the total number of two- and higher-fold events acquired during the experiment, around 80%, amounting to 2.1×10^9, was from the deexcitation of ^{82}Kr. The data were sorted into γ-γ matrices, symmetric as well as angle dependent, and γ-γ-γ cube using the MARCOS [29] code and analyzed using the INGASORT [30] and the RADWARE [31,32] packages.

We have observed 975.2-, 1673.7-, 696.9-, 1395.3-, and 1113.6-keV E2 transitions in the low-lying structure of ^{82}Kr (Fig. 1), for the first time in heavy-ion reactions, which were previously seen in β decay of ^{82}Rb [33,34]. Apart from these, a total of nine new γ transitions of energies 629.8, 846.0, 1100.2, 1209.5, 1211.3, 1219.3, 1274.6, 1473.4, and 1810.6 keV and five new levels at 3194, 3765, 4405, 4560, and 4759 keV have been identified from the investigation. Measured directional correlation from oriented states (DCO) ratios and polarization values of γ-ray transitions have been used to extract the mixing ratio (δ) of the mixed $M1/\mathrm{E2}$ transitions

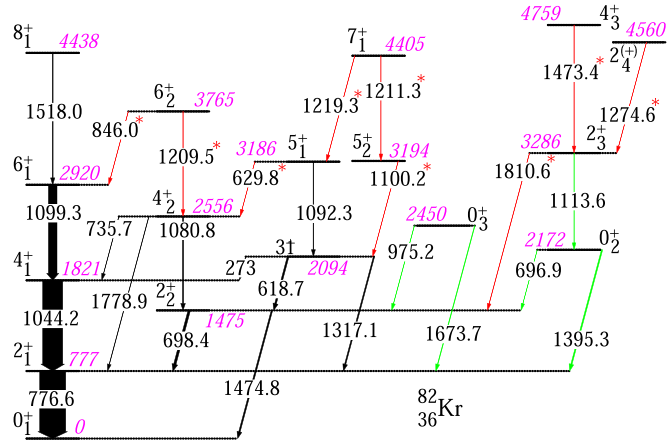

FIG. 1. The partial level scheme of ^{82}Kr obtained in the present Letter. The level energies (represented by the magenta-colored numbers) are rounded off to the nearest keV. The newly observed transitions have been red colored (marked by "∗'s") whereas green-colored transitions have been first observed in heavy-ion reactions and were seen previously in β decay of ^{82}Rb [33,34]. Here, the indexing is just for the states observed in this experiment, and there are additional 0^+, 2^+, and 4^+ levels that were observed previously in ^{82}Kr.

by comparing their theoretical values (Fig. 2). The analysis has been validated with the previously known/measured 618.7-, 698.4-, and 1317.1-keV transitions for which the δ from the present measurement overlap with the literature values [35]. The procedure has, thus, been extended to the 629.8-, 735.7-, and 1810.6-keV transitions that are newly identified herein and results are recorded in Table I. For the 273.0-, 696.9-, 846.0-keV transitions, only the DCO ratios could be extracted and corresponding assignments of these transitions were confirmed through the definitive spin parity of the

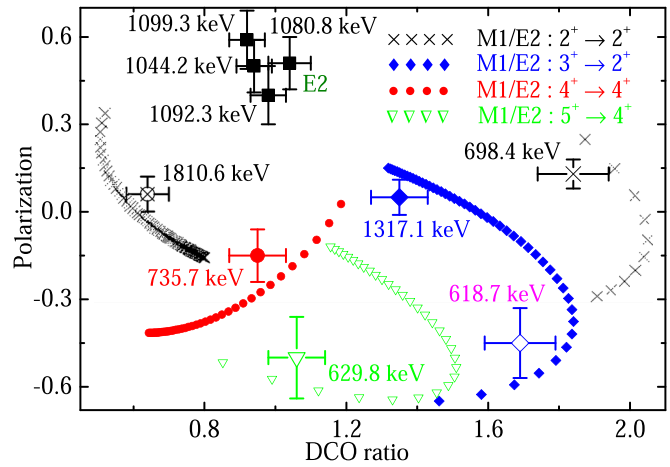

FIG. 2. Experimental (symbols with X and Y error bars) and calculated (represented by ×, •, ♦, and ▽ symbols) DCO ratio and linear polarization values for different multipole mixing ratio (δ) of the transitions in ^{82}Kr. E2 gates set on the 140° and 90° detectors to extract DCO ratios whereas 90° detectors used for the linear polarization measurements.

TABLE I. γ-energy (E_γ), assignment ($\sigma\lambda$), branching (Br), mixing ratio (δ), lifetimes, and the corresponding B(E2) transitions rates for the low-lying states in ^{82}Kr. Uncertainties of the measured values are rounded off to the next first decimal place. Quoted errors of the B(E2) values include the uncertainty due to the δ (for $M1$/E2 transitions only), Br, and lifetime measurements.

I^π ($\hbar$)	E_γ (keV)	$\sigma\lambda$	Br (%)	δ	Lifetime (ps)	B(E2) (W.u.)
2_1^+	776.6	E2	100.0		6.4(3)[a]	21.3(10)[a]
4_1^+	1044.2	E2	100.0		1.0(1)	31.1(31)
2_2^+	698.4	$M1$/E2	62.0(9)	0.6(1)	1.1(1)	34.6(63)
	1474.8	E2	38.0(9)			1.9(2)
6_1^+	1099.3	E2	100.0		0.7(1)	34.3(49)
4_2^+	1080.8	E2	64.1(13)		1.0(1)	16.8(17)
	1778.9	E2	20.9(13)			0.5(1)
	735.7	$M1$/E2	15.0(13)	1.2(3)		15.8(45)
3_1^+	1317.1	$M1$/E2	41.2(13)	3.7(7)	3.9(5)	1.0(2)
	618.7	$M1$/E2	57.0(13)	0.9(2)		27.8(72)
	273.0	$M1$/E2	1.8(13)	0.3(1)		9.7(75)
8_1^+	1518.0	E2	100.0		0.2 ↓[b]	23.9 ↑[b]
6_2^+	1209.5	E2	58.7(12)		0.4 ↓[b]	21.9 ↑[b]
	846.0	$M1$/E2	41.3(12)	0.3(1)		7.6 ↑[b]
5_1^+	1092.3	E2	83.6(17)		1.2(1)	17.3(15)
	629.8	$M1$/E2	16.4(17)	0.4(1)		7.3(18)
7_1^+	1219.3	E2	56.6(20)		0.2 ↓[b]	40.5↑[b]
	1211.3	E2	43.4(20)			32.1 ↑[b]
0_3^+	1673.7	E2	48.4(22)			
	975.2	E2	51.6(22)			
0_2^+	1395.3	E2	99.5(10)		0.6(1)	12.1(20)
	696.9	E2	0.5(10)			2.0(40)
2_3^+	1113.6	E2	28.1(21)		0.5(1)	12.7(27)
	1810.6	$M1$/E2	71.9(21)	$-2.8^{+0.9}_{-1.4}$		$2.5^{+0.8}_{-1.1}$
4_3^+	1473.4	E2	100.0		0.3 ↓[b]	18.5 ↑[b]
$2_4^{(+)}$	1274.6	$M1$/E2	100.0	+2.9(7)	0.5 ↓[b]	20.5 ↑[b]

[a]Adopted from Ref. [27].
[b]↑ and ↓ represent lower and upper limits, respectively.

respective initial and final states. The low-lying structure of ^{82}Kr (Fig. 1) relevant to this Letter is obtained by accumulating the extracted spectroscopic information and overlaps with the previously reported ones [27,33,34,36,37].

In accordance with the principal objective of this Letter, lifetimes have been determined for 13 levels in ^{82}Kr using the Doppler shift attenuation method (DSAM). The lifetime analysis has been carried out using an updated methodology reported by Das *et al.* [38]. The same pertains to incorporating the evolving yield of the recoils with changing beam energy, across the thickness of the target, whereas simulating the velocity profiles, and using these to calculate the Doppler shapes on the transition peaks. The calculation of the shapes and their least square fitting to the experimental spectra are implemented through the use of the LINESHAPE [39,40] package. As has been reported by Das *et al.* [38], the stopping trajectories are based on the simulations using TRIM [28] whereas the energy-angle distribution of the recoils at different beam energies are calculated using the PACE code [41,42].

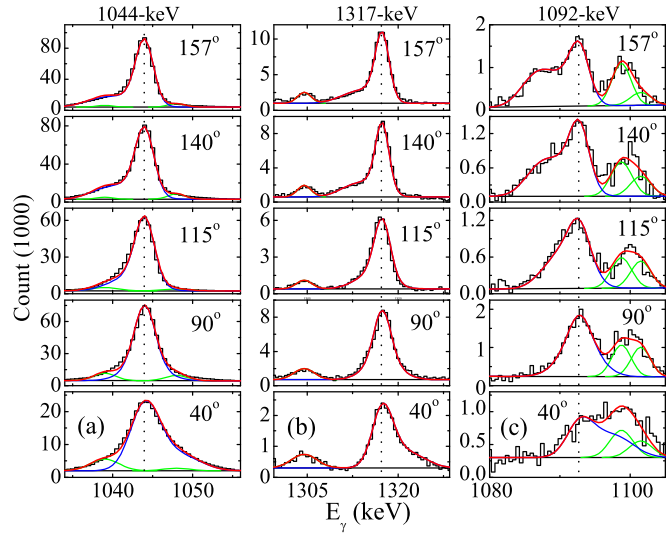

FIG. 3. Experimental spectra created by the gate on top of the transition along with the fitted Doppler shapes (total in red and deconvoluted in blue), contaminant (stopped) peaks (in green), and background (as a black solid line) for the (a) 1044.2-, (b) 1317.1-, and (c) 1092.3-keV transitions in ^{82}Kr. The vertical dotted lines represent the stopped peak position of the transition.

Lifetimes for most of the levels have been extracted from analysis of spectra corresponding to the appropriate gate on top (GTT) as well as the gate on below the transition (GTB) of interest. The analysis carried out with the GTT spectra is known to be unaffected by any side-feeding contribution to the level of interest. However, the lifetimes could not be extracted with GTT for the 7_1^+, 8_1^+, 6_2^+, 2_3^+, 2_4^+, and 4_3^+ states. In GTB, the contribution from the side-feeding transitions is modeled with a cascade of five transitions whose moment of inertia is assumed to be similar to the band of interest. In this process, the effect of variation in the side-feeding intensity resulted in a change in the evaluated level lifetime by less than 10%. The Doppler shapes (observed) at five different angles have been fitted simultaneously to extract the lifetime (Fig. 3). Table I summarizes the lifetime results along with the B(E2) values of the levels in ^{82}Kr. The quoted uncertainties do not include the systematic contribution ($\approx$5%) of the stopping powers, that have been extracted from the SRIM [28] software with updated and experimentally validated results. The analysis procedure is further detailed in Refs. [43,44].

Previously reported level lifetimes of the ground-state band in ^{82}Kr were in agreement with thepresent measurement except for the 6_1^+ state. For this state, our lifetime $0.7^{+0.1}_{-0.1}$ ps though deviates from the value (4^{+2}_{-1} ps) reported by Kemnitz *et al.* [27] but overlapped with the lifetime $1.2^{+1.4}_{-0.4}$ ps obtained from the Coulomb excitation study [36]. The deviation from Kemnitz *et al.* [27] is due to the long lifetime of the 8_1^+ state which dominates the decay function of the 1099.3-keV transition ($6_1^+ \rightarrow 4_1^+$) as discussed in Ref. [36].

The ^{82}Kr nucleus has eight proton particles and four neutron holes with respect to the doubly magic ^{78}Ni ($Z = 28$ and $N = 50$) [45] and is, thus, presumably away from the U(5) paradigm. Indeed, $B(\text{E2}: 2_1^+ \rightarrow 0_1^+)$ rates along the isotopic

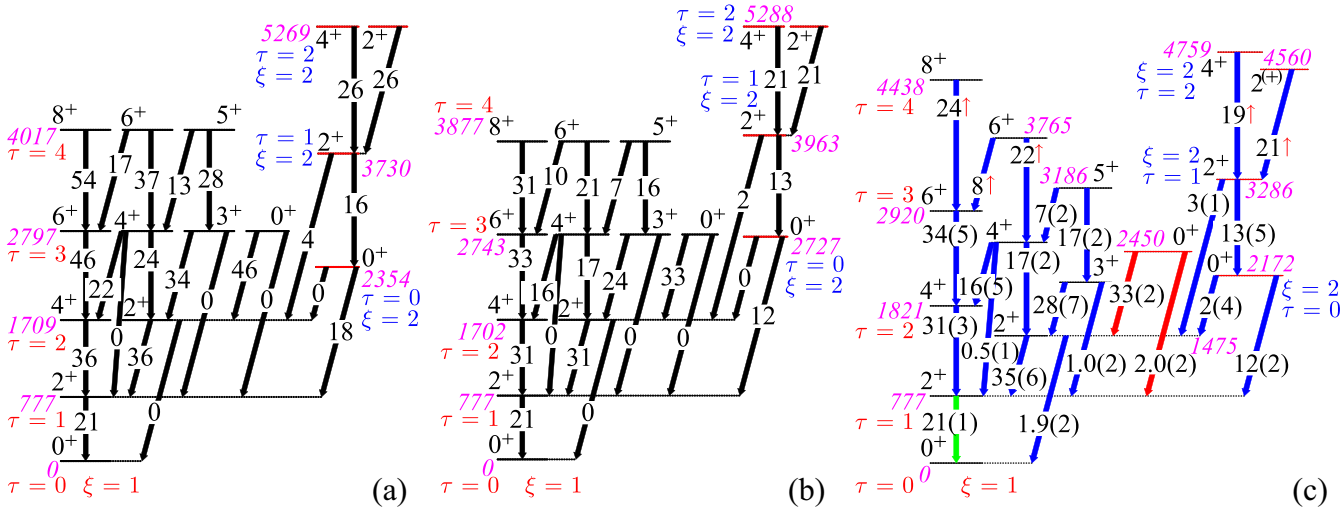

FIG. 4. Level scheme of the E(5) symmetry ($\tau = 0$–4 levels of $\xi = 1$ family and the $\tau = 0$–2 levels with $\xi = 2$) for (a) infinite-N_B and (b) $N_B = 6$ in the IBA calculation compared with (c) the level scheme of ^{82}Kr that was obtained experimentally. Width of the transitions represents B(E2) values in the Weisskopf units (W.u.s) and normalized with the measured value of $B(\mathrm{E2}: 2^+_{1,1} \rightarrow 0^+_{1,0}) = 21.3$ W.u. In (c) present measurements are colored by blue whereas green-colored one adopted from Ref. [27]. Branching ratio of the $0^+_{1,3}$ level is normalized with $B(\mathrm{E2}: 0^+_{1,3} \rightarrow 2^+_{1,2}) = 33$ W.u. (IBA calculation for $N_B = 6$), and the depopulating transitions from this state are colored by red. The level energies both for the experimental and calculated scheme are rounded off to the nearest keV (represented by the magenta-colored numbers).

chain of Kr ($A = 74$–84) [19,20,25–27,36,46,47] indicate that ^{82}Kr is located in the transition region between the O(6) and the U(5) limits. In order to probe the E(5) dynamical symmetry in ^{82}Kr, we have performed the IBA calculations by adopting the Hamiltonian $H = \epsilon n_d + \mathrm{AP}^\dagger\mathrm{P}$, where ϵ and A are the parameters at the critical point on the U(5) to O(6) path, defined by ratio $\epsilon/A = 2(N_B - 1) = 10$ for $N_B = 6$, N_B being the boson number [48]. The first term of H gives the unperturbed energy of a state with n_d noninteracting d bosons whereas the second term provides the energy due to the pairing interaction. Energy levels of the system in the E(5) model are characterized by quantum numbers ξ and τ [8]. Here, $\xi = 1$–3, ... represents major families whereas τ denotes the phonon excitationlike levels within a ξ family ($\tau = 0$–2, ...). Henceforth, we will designate the levels by their (ξ, τ) quantum numbers, e.g., the 2^+_1, 4^+_1, and 2^+_2 states with quantum numbers $\xi = 1$, $\tau = 1$, 2, and 2 will be labeled as $\xi = 1$, $\tau = 1$, 2, and $2^+_{1,2}$, respectively.

Figure 4(a) illustrates good agreement of the (experimental) level energies and the associated B(E2) values in ^{82}Kr with the predictions of the E(5) symmetry for the infinite N_B [8]. Figure 4(b) represents the (IBA) calculated level energies and the B(E2) values corresponding to $N_B = 6$ along with an adjusted scale parameter $\epsilon = 1.30$. Although the calculated level energies therefrom exhibit reasonable overlap with the experimental ones, the B(E2) values from the (present) measurement are in excellent compliance with those from the calculations normalized with $B(\mathrm{E2}: 2^+_{1,1} \rightarrow 0^+_{1,0}) = 21.3$ W.u. Also, measured B(E2) values are in good agreement with those predicted for E(5) as described in Refs. [13,49,50]. These observations collectively indicate the existence of E(5) dynamical symmetry in ^{82}Kr.

It follows from the excitation scheme of ^{82}Kr, Figs. 1 and 4(c), the 0^+_3 state at 2450 keV has a large B(E2) value to the $2^+_{1,2}$ state *vis á vis* the $2^+_{1,1}$ state and has, thus, been identified to be the $0^+_{1,3}$ level. The 0^+_2 level at 2172 keV shows a preferred decay to the $2^+_{1,1}$ state, indicating that it might be associated with the band head of the $\xi = 2$ family of levels, and, thus, the state is assigned as $0^+_{2,0}$. Measured values $\frac{B(E2: 0^+_{2,0} \rightarrow 2^+_{1,2})}{B(E2: 0^+_{2,0} \rightarrow 2^+_{1,1})} = 0.2(3)$, $\frac{B(E2: 0^+_{1,3} \rightarrow 2^+_{1,1})}{B(E2: 0^+_{1,3} \rightarrow 2^+_{1,2})} = 0.1(1)$, $\frac{E(0^+_{1,3})}{E(2^+_{1,1})} = 3.2$, and $\frac{E(0^+_{2,0})}{E(0^+_{1,3})} = 0.9$ are in satisfactory agreement with the IBA predictions, 0.00, 0.00, 3.53, and 0.99, respectively. These observations further corroborate the assignment of the 2172- and 2450-keV states as the $0^+_{2,0}$ and $0^+_{1,3}$ levels of E(5) dynamical symmetry, respectively.

One of the most striking findings in the context of E(5) symmetry in ^{82}Kr is the identification of the excited $2^+_{2,1}$, $2^+_{2,2}$, and $4^+_{2,2}$ states at 3286, 4560, and 4759 keV, respectively, above the $0^+_{2,0}$ state of the $\xi = 2$ family and measurement of their B(E2) rates as depicted in Fig. 4(c) and Table I. The $2^+_{2,2}$ state, band head of the γ band for the second ξ family, is observed very close in the energy of the $4^+_{2,2}$ level, thus, adds extra weightage in the proposed symmetry. All these excited states have not been observed in the previously identified candidates of E(5) [11–14]. It is worth noting that the measured transition probability ratios of $B_{020\rightarrow 211} = \frac{B(\mathrm{E2}: 0^+_{2,0} \rightarrow 2^+_{1,1})}{B(\mathrm{E2}: 2^+_{1,1} \rightarrow 0^+_{1,0})} = 0.6(1)$, $B_{221\rightarrow 020} = \frac{B(\mathrm{E2}: 2^+_{2,1} \rightarrow 0^+_{2,0})}{B(\mathrm{E2}: 2^+_{1,1} \rightarrow 0^+_{1,0})} = 0.6(1)$, $B_{221\rightarrow 212} = \frac{B(\mathrm{E2}: 2^+_{2,1} \rightarrow 2^+_{1,2})}{B(\mathrm{E2}: 2^+_{1,1} \rightarrow 0^+_{1,0})} = 0.1(1)$, and $B_{422\rightarrow 221} = \frac{B(\mathrm{E2}: 4^+_{2,2} \rightarrow 2^+_{2,1})}{B(\mathrm{E2}: 2^+_{1,1} \rightarrow 0^+_{1,0})} = 0.9\uparrow$, $B_{222\rightarrow 221} = \frac{B(\mathrm{E2}: 2^+_{2,2} \rightarrow 2^+_{2,1})}{B(\mathrm{E2}: 2^+_{1,1} \rightarrow 0^+_{1,0})} = 1.0\uparrow$ as well as the excitation energies $\frac{\mathrm{E}(2^+_{2,1})}{\mathrm{E}(2^+_{1,1})} = 4.2$ and $\frac{\mathrm{E}(4^+_{2,2})}{\mathrm{E}(2^+_{1,1})} = 6.1$ values are reproduced well in the IBA calculations that output the corresponding values as 0.56, 0.61, 0.11, 0.94, 0.94, 5.10, and 6.80, respectively.

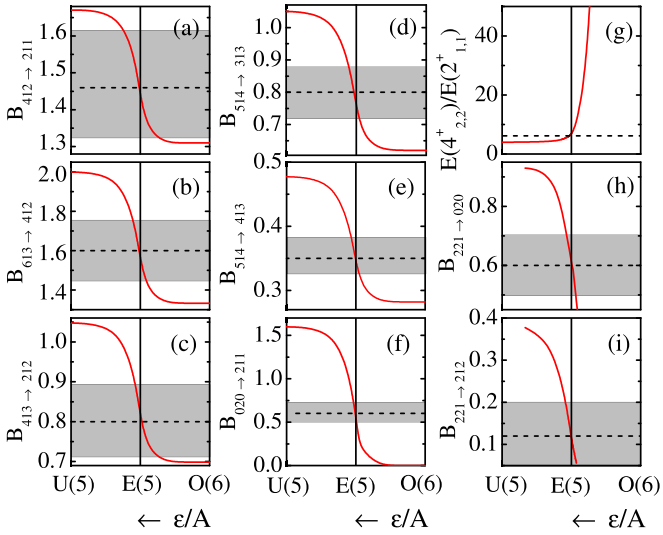

FIG. 5. Variation (represented by red solid curves) of (a) $B_{412\to211}$, (b) $B_{613\to412}B_{613\to412}$, (c) $B_{413\to212} = \frac{B(E2:4^+_{1,3}\to2^+_{1,2})}{B(E2:2^+_{1,1}\to0^+_{1,0})}$, (d) $B_{514\to313} = \frac{B(E2:5^+_{1,4}\to3^+_{1,3})}{B(E2:2^+_{1,1}\to0^+_{1,0})}$, (e) $B_{514\to413} = \frac{B(E2:5^+_{1,4}\to4^+_{1,3})}{B(E2:2^+_{1,1}\to0^+_{1,0})}$, (f) $B_{020\to211}$, (g) $\frac{E(4^+_{2,2})}{E(2^+_{1,1})}$, (h) $B_{221\to020}$, and (i) $B_{221\to212}$ from U(5), through E(5) (denoted by vertical solid lines), to O(6) against the ratio ϵ/A. ϵ/A values for U(5), E(5), and O(6) are ∞, 10, and 0, respectively. Experimental values and uncertainty ranges are indicated by the horizontal dashed lines and shaded rectangles, respectively.

The (IBA) calculated values of these different observables have been plotted against the ϵ/A in Fig. 5 and compared with the measured ones. It follows that the calculations reproduce the measured values at $\epsilon/A = 10$ corresponding to the E(5) paradigm and cater for an assertive evidence of E(5) dynamical symmetry in ^{82}Kr.

To further illustrate the phase-transitional behavior in ^{82}Kr, we have performed IBA calculations within the "consistent Q formalism" using the Hamiltonian [1],

$$H = \epsilon n_d - kQ^\dagger Q = C\left[(1-\zeta)n_d - \frac{\zeta}{4N_B}Q^\dagger Q\right], \quad (1)$$

where $\zeta = \frac{4N_B}{4N_B+\epsilon_d/k}$ and C is a normalization constant that only scales the energies. In this calculation two significant parameters ζ (varies from 0 to 1) and χ (varies from $-\sqrt{7}/2$ to 0) are used with $N_B = 6$. The key experimental observables, such as $B_{412\to211} = \frac{B(\mathrm{E2}:\,4^+_{1,2}\to2^+_{1,1})}{B(\mathrm{E2}:\,2^+_{1,1}\to0^+_{1,0})}$, $B_{613\to412} = \frac{B(\mathrm{E2}:\,6^+_{1,3}\to4^+_{1,2})}{B(\mathrm{E2}:\,2^+_{1,1}\to0^+_{1,0})}$, $B_{020\to211}$, $B_{221\to020}$, $B_{221\to212}$ and $\frac{\mathrm{E}(4^+_{2,2})}{\mathrm{E}(2^+_{1,1})}$, are reproduced for $\zeta = 0.60$ and $\chi = 0$ that actually represent the exact E(5) dynamical symmetry [51] and upholds that ^{82}Kr exemplifies the second-order phase-transitional point in the evolution from U(5) to O(6) domains of nuclear structure. This is also an example wherein a nucleus has been identified to represent a CPS so closely and is expected to indicate pathways for further studies in this domain.

To summarize, low-lying positive-parity states in ^{82}Kr are investigated using heavy-ion-induced fusion-evaporation reaction and a large array of Compton suppressed clover detectors. Apart from other spectroscopic measurements, level lifetimes are extracted using the DSAM and transition probabilities have been determined therefrom. Energies and the B(E2) values of the relevant states in ^{82}Kr exhibit striking agreement with the IBA and the E(5) model calculations. Evidence of E(5) dynamical symmetry in ^{82}Kr is identified uniquely through the maiden measurement of energy and B(E2) rates for the structure of the second ξ family, observed for the first time, and their comparison with the calculations. It can, thus, be asserted that the ^{82}Kr nucleus represents the critical point of phase (shape) transition between U(5) and O(6) paradigms. This finding adds to the very limited observations existing for E(5) symmetry in $A < 100$ nuclei and, in fact, is the only instance wherein the properties of a nucleus have been unraveled to be so proximal to those predicted for a critical point. It is envisaged that such studies will facilitate a better understanding of nuclear properties accompanying the phase (shape) transitions and contribute towards developing a systematic model of the same.

We acknowledge the help and support from the INGA Collaboration. We remain grateful to Prof. R. F. Casten (Yale) for stimulating and fruitful discussions. We thank Prof. S. Chattopadhyay (SINP) for providing the target material of the experiment [52]. We are thankful to the staff at the Pelletron LINAC Facility in TIFR for their efforts in delivering steady and uninterrupted ^{9}Be beam. We gratefully acknowledge financial support by the Department of Science and Technology (DST) for the INGA Project (Project No. IR/S2/PF-03/2003-II). H.P. is grateful for the support of the Ramanujan Fellowship Research Grant under SERB-DST Grant No. (SB/S2/RJN-031/2016). H.P. is also grateful for the fruitful discussion with Prof. Dr. N. Pietralla (TU-Darmstadt). S.R. would like to acknowledge financial assistance from the UGC-DAE Consortium for Scientific Research, Kolkata Centre under the Collaborative Research Scheme (CRS) (Grant No. UGC-DAE-CSR/KC/CRS/19/NP13/0924) and the FRPDF Grant of Presidency University, Kolkata, India. S.B. would like to acknowledge financial assistance from the UGC-DAE-CSR Project (Project No. UGC-DAE-CSR-KC/CRS/19/NP04/0915) and the IUAC Project (Project No. IUAC/XIII.3A/UFR-55313).

[1] R. F. Casten, Nat. Phys. **2**, 811 (2006).
[2] R. F. Casten and E. A. McCutchan, J. Phys. G: Nucl. Part. Phys. **34**, R285 (2007).
[3] G. Sharff-Goldhaber and J. Weneser, Phys. Rev. **98**, 212 (1955).
[4] A. Bohr and B. R. Mottelson, Phys. Rev. **90**, 717 (1953).
[5] L. Wilets and M. Jean, Phys. Rev. **102**, 788 (1956).
[6] F. Iachello and A. Arima, *The Interacting Boson Model* (Cambridge University Press, Cambridge, UK, 1987).

[7] F. Iachello, Phys. Rev. Lett. **87**, 052502 (2001).
[8] F. Iachello, Phys. Rev. Lett. **85**, 3580 (2000).
[9] J. Meng, W. Zhang, S. G. Zhou, H. Toki, and L. S. Geng, Eur. Phys. J. A **25**, 23 (2005).
[10] J. Y. Guo, Int. J. Mod. Phys. E. **17**, 539 (2008).
[11] R. F. Casten and N. V. Zamfir, Phys. Rev. Lett. **85**, 3584 (2000).
[12] Z. Da-Li and L. Yu-Xin, Chin. Phys. Lett. **20**, 1028 (2003).
[13] A. Frank, C. E. Alonso, and J. M. Arias, Phys. Rev. C **65**, 014301 (2001).
[14] N. V. Zamfir, M. A. Caprio, R. F. Casten, C. J. Barton, C. W. Beausang, Z. Berant, D. S. Brenner, W. T. Chou, J. R. Cooper, A. A. Hecht, R. Krücken, H. Newman, J. R. Novak, N. Pietralla, A. Wolf, and K. E. Zyromski, Phys. Rev. C **65**, 044325 (2002).
[15] R. M. Clark, M. Cromaz, M. A. Deleplanque, M. Descovich, R. M. Diamond, P. Fallon, I. Y. Lee, A. O. Macchiavelli, H. Mahmud, E. Rodriguez-Vietez, F. S. Stephens, and D. Ward, Phys. Rev. C **69**, 064322 (2004).
[16] L. Coquard, N. Pietralla, T. Ahn, G. Rainovski, L. Bettermann, M. P. Carpenter, R. V. F. Janssens, J. Leske, C. J. Lister, O. Möller, W. Rother, V. Werner, and S. Zhu, Phys. Rev. C **80**, 061304(R) (2009).
[17] D. Bonatsos, D. Lenis, N. Pietralla, and P. A. Terziev, Phys. Rev. C **74**, 044306 (2006).
[18] N. Marginean *et al.*, Phys. Lett. B **633**, 696 (2006).
[19] H. Rotter *et al.*, Nucl. Phys. A **514**, 401 (1990).
[20] J. Keinonen *et al.*, Atom. Data Nucl. Data Tables **36**, 1 (1987).
[21] E. A. Stefanova, R. Schwenger, J. Reif, H. Schnare, F. Dönau, M. Wilhelm, A. Fitzler, S. Kasemann, P. von Brentano, and W. Andrejtscheff, Phys. Rev. C **62**, 054314 (2000).
[22] E. K. Warburton, J. W. Olness, C. J. Lister, R. W. Zurmühle, and J. A. Becker, Phys. Rev. C **31**, 1184 (1985).
[23] M. Hannawald, T. Kautzsch, A. Wöhr, W. B. Walters, K.-L. Kratz, V. N. Fedoseyev, V. I. Mishin, W. Böhmer, B. Pfeiffer, V. Sebastian, Y. Jading, U. Köster, J. Lettry, H. L. Ravn, and ISOLDE Collaboration, Phys. Rev. Lett. **82**, 1391 (1999).
[24] E. Caurier, F. Nowacki, and A. Poves, Eur. Phys. J. A **15**, 145 (2002).
[25] H. Iwasaki *et al.*, Phys. Rev. Lett. **112**, 142502 (2014).
[26] A. Görgen *et al.*, Eur. Phys. J. A **26**, 153 (2005).
[27] P. Kemnitz *et al.*, Nucl. Phys. A **425**, 493 (1984).
[28] J. F. Ziegler, M. D. Ziegler, and J. P. Biersack, Nucl. Instrum. Methods. Phys. Res. B **268**, 1818 (2010).
[29] R. Palit *et al.*, Nucl. Instrum. Methods Phys. Res. Sect. A **680**, 90 (2012).
[30] R. K. Bhowmik, Ingasort Manual (private communication).
[31] D. C. Radford, Nucl. Instrum. Methods Phys. Res. Sect. A **361**, 297 (1995).
[32] D. C. Radford, Nucl. Instrum. Methods Phys. Res. Sect. A **361**, 306 (1995).
[33] M. N. Nino, E. A. McCutchan, S. V. Smith, C. J. Lister, J. P. Greene, M. P. Carpenter, L. Muench, A. A. Sonzogni, and S. Zhu, Phys. Rev. C **93**, 024301 (2016).
[34] R. A. Meyer, J. F. Wild, K. Eskola, M. E. Leino, S. Väisälä, K. Forssten, U. Kaup, and A. Gelberg, Phys. Rev. C **27**, 2217 (1983).
[35] J. K. Tuli and E. Browne, Nucl. Data Sheets **157**, 260 (2019).
[36] S. Brüssermann, K. P. Lieb, P. Sona, H. Emling, E. Grosse, and J. Stachel, Phys. Rev. C **32**, 1521 (1985).
[37] A. Zemel, T. Hageman, J. J. Hamill, and J. van Klinken, Phys. Rev. C **31**, 1483 (1985).
[38] S. Das *et al.*, Nucl. Instrum. Methods Phys. Res. Sect. A **841**, 17 (2017).
[39] J. C. Wells and N. R. Johnson, LINESHAPE: A Computer Program for Doppler Broadened Lineshape Analysis, Oak Ridge National Laboratory Report No. ORNL-6689, 44, 1991 (unpublished).
[40] N. R. Johnson, J. C. Wells, Y. Akovali, C. Baktash, R. Bengtsson, M. J. Brinkman, D. M. Cullen, C. J. Gross, H.-Q. Jin, I.-Y. Lee, A. O. Macchiavelli, F. K. McGowan, W. T. Milner, and C.-H. Yu, Phys. Rev. C **55**, 652 (1997).
[41] A. Gavron, Phys. Rev. C **21**, 230 (1980).
[42] O. B. Tarasov and D. Bazin, Nucl. Instrum. Methods. Phys. Res. B **266**, 4657 (2008).
[43] S. Rajbanshi, Abhijt Bisoi, Somnath Nag, S. Saha, J. Sethi, T. Trivedi, T. Bhattacharjee, S. Battacharyya, S. Chattopadhyay, G. Mukherjee, R. Palit, R. Raut, M. Saha Sarkar, A. K. Singh, and A. Goswami, Phys. Rev. C **89**, 014315 (2014).
[44] S. Rajbanshi, Abhijit Bisoi, Somnath Nag, S. Saha, J. Sethi, T. Bhattacharjee, S. Bhattacharyya, S. Chattopadhyay, G. Gangopadhyay, G. Mukherjee, R. Palit, R. Raut, M. Saha Sarkar, A. K. Singh, T. Trivedi, and A. Goswami, Phys. Rev. C **90**, 024318 (2014).
[45] R. Taniuchi *et al.*, Nature (London) **569**, 53 (2019).
[46] P. K. Joshi *et al.*, Nucl. Phys. A **700**, 59 (2002).
[47] L. Funke *et al.*, Nucl. Phys. A **355**, 228 (1981).
[48] A. E. L. Dieperink, O. Scholten, and F. Iachello, Phys. Rev. Lett. **44**, 1747 (1980).
[49] J. M. Arias, Phys. Rev. C **63**, 034308 (2001).
[50] M. A. Caprio, Phys. Rev. C **65**, 031304(R) (2002).
[51] V. Werner *et al.*, Phys. Lett. B **527**, 55 (2002).
[52] See Supplemental Material at https://link.aps.org/supplemental/10.1103/PhysRevC.104.L031302 for further details on the data analysis.